Journal Pre-proofs

Second-order fatigue of intrinsic mean stress under random loadings

Iñigo Calderón-Urízsar-Aldaca, María Victoria Biezma, Amaia Matanza, Estibaliz Briz, David M. Bastidas

PII: S0142-1123(19)30361-5
DOI: https://doi.org/10.1016/j.ijfatigue.2019.105257
Reference: JIJF 105257

To appear in: *International Journal of Fatigue*

Received Date: 10 July 2019
Revised Date: 26 August 2019
Accepted Date: 28 August 2019

Please cite this article as: Calderón-Urízsar-Aldaca, I., Biezma, M.V., Matanza, A., Briz, E., Bastidas, D.M., Second-order fatigue of intrinsic mean stress under random loadings, *International Journal of Fatigue* (2019), doi: https://doi.org/10.1016/j.ijfatigue.2019.105257

Second-order fatigue of intrinsic mean stress under random loadings

Iñigo Calderón-Urízsar-Aldaca[a], María Victoria Biezma[b], Amaia Matanza[c], Estibaliz Briz[d], David M. Bastidas[e]

[a]*Sustainable Construction Division, Tecnalia Research and Innovation, 20009 San Sebastian, Guipuzcoa, Spain*
[b]*Department of Earth and Materials Science and Engineering, University of Cantabria, 39004 Santander. Spain*
[c]*SIAME - MPC (UPV/EHU) Universit de Pau et des pays de l'Adour ISA BTP, 64600 Anglet, France.*
[d]*Department of Mechanical Engineering, University of the Basque Country (UPV/EHU), 48940 Leioa, Vizcaya, Spain*
[e]*National Center for Education and Research on Corrosion and Materials Performance, NCERCAMP-UA. Dept. Chemical, Biomolecular, and Corrosion Engineering. The University of Akron, 302 E Buchtel Ave, Akron, OH 44325-3906, United States.*

Abstract

A fatigue process due to random loading that is progressively damaging a certain structural detail will vary in the presence of mean stresses. The variations are already considered in crack propagation laws and by applying equivalent 0-mean stress ranges from the Palmgren-Miner linear rule. Nevertheless, if the mean stress is intrinsic, instead of a direct consequence of the random loading, other second-order effects will have to be taken into account. Those effects are cycle quasi-ordering, histogram variations, and apparent mean tension, which are identified and defined in this study and, finally, developed in a case study for demonstrative purposes.

Keywords: Random loading, mean stress, second-order, fatigue damage

1. Introduction

Mean stress, σ_m, is a factor that can be determinate in fatigue. Its clear influence on the ultimate number of cycles, N_f, that a certain structural element or *detail* can withstand up until failure under *ceteris paribus* conditions, in terms

of the stress range, $\Delta\sigma$, and the cycle amplitude, has repeatedly been identified over recent years [1, 2, 3, 4, 5].

Nevertheless, fatigue in practical structural engineering is still studied by means of the Palmgren-Miner linear rule [6, 7], which incorporates Wöhler curves [8]. Those curves are specified in standards such as the Eurocodes [9, 10, 11] derived from ECCS seminal work [12] and in various other standards: AISC, ASCE, and AASTHO [13, 14, 15, 16, 17]. They are linearized in Basquin's Law [18] as a log-log ratio, which also neglects the mean tension effect, as the curves are derived by testing under totally reversed loading conditions, i.e. with zero mean tension, $\sigma_m = 0$.

Moreover, the alternative theoretical procedure, see [12], based on Paris' Law [19] with a failure criteria, also neglects mean stress. Examples are the procedures first proposed by Griffith [20] and Irwin [21], for analytical forecasts of fatigue failure by studying crack propagation. In fact, it is only considered when setting the stress intensity threshold, K_{th}, and the critical K_{cr} values. In other words, mean stress sets the initial or threshold crack size, a_{th}, and the final or critical crack sizes, a_{cr}, but it is not included in crack-propagation calculations between both points.

For instance, when referring to the crack propagation rate per cycle, da/dN, in fatigue processes under axial tension, crack propagation will tend to run in a perpendicular direction to tension, while it will tend to propagate in parallel to axial compression. Hence, different geometric factors, such as $Y(a)$ in Paris' law [19], will reflect different stress concentration laws and so on. It is therefore not a simple matter that is only limited to crack thresholds and critical sizes. Latest studies, like *Choi et Al.* [22] or *Chandran* [23], are considering mean stress in crack propagation models in deep consideration on this subject.

2. Extrinsic and intrinsic mean stresses

As already known, the term *mean stress* in a certain fatigue cycle refers to the stress value that is precisely midway between the minimum and the maximum

stress values.

Thus, in structural engineering, typical dynamic loads such as wind, seismic activity, traffic, machine and human induced vibrations among others, tend to cause time-dependent forces, or actions, that proportionally induce time-dependent stresses in the corresponding structural details [24, 16, 13]. Those forces are independent of the structures, at least when disregarding non-linear interactions such as aeroelasticity, and will therefore tend to to be studied accordingly. For instance, a cycle corresponding to a wind pressure variation from $1 \cdot kN/m^2$ to $2 \cdot kN/m^2$ that causes a stress cycle. The mean stress, σ_m, of that stress cycle is produced by a mean pressure of $1.5 \cdot kN/m^2$ with a stress range, $\Delta\sigma$, that is produced by a pressure variation of $1 \cdot kN/m^2$, regardless of the concomitant mean stress. Hence, this decomposition is still suitable within the framework of the superposition principle in continuum mechanics, applied to a *Hookean* body under a linear elastic range, according to the theory of elasticity [25], and precisely in the case of *high-cycle fatigue*.

Thus, some cycle counting methods in the state-of-the-art, such as the widely known *Rainflow* method [26], the most accurate according to [27], its direct derivatives [28, 29], its evolutions such as the *3-point* ASTM rule [30, 31, 32], the *4-point* modification [33], the *recursive* algorithm [34], and closer counting methods such as the *Reservoir* [11], are used to extract the stress range histograms of complex random dynamic loads, while keeping the information of the mean stress of each cycle [35]. They are then directly calculated in either the *time domain* by a simple quasi-static calculation or in the *frequency domain* with, for example, the *Tovo-Benasciutti* method [36, 37], which uses the such mean-stress information of each cycle, among several other methods, see Mrsnik [38].

Hence, following the plain *time domain* calculation, each characteristic range interval in the histogram is cross referenced with its corresponding stress range. Then, with the number of cycles, the fatigue is calculated with the Palmgren-Miner [6, 7] linear rule and the corresponding Wöhler curve [8].

The alternative is to use the *frequency domain*, a procedure that will now

be briefly reviewed. It starts by deriving the *Power Spectral Density* (PSD) function of a certain random dynamic action with a first *Fast Fourier Transformation* (FFT) or *Direct Fourier Transformation* (DFT), passing from the time domain to the frequency domain. It is then transposed into the structural response PSD with the use of the *Frequency Response Functions* (FRF) of the Multi-Degree of Freedom (MDOF) system, with lumped masses and considering dynamic stationary and ergodic action [39, 40, 41]. Then, the stresses are derived from the displacements and the superposition principle of elasticity. In that way, the expected number of cycles per second is the root square of the 4th-order moment divided by the 2nd-order moment of the response PSD function. The expected fatigue damage can be derived by means of some methods that retain mean stress and ranges, such as the *Tovo-Benasciutti* method, among others [38].

However, that fatigue calculation method only takes into account the effect of the dynamic load cycle mean stress. It is therefore not conservative when considering sources of mean stress in other elements. The approach is furthermore based on *extrinsic mean stress*, implying that the source of mean stress is from the exterior of the structure.

For instance, elements with concomitant permanent tensile loading, such as prestressed bolts, tendons, cables, rods, and beams under tension, among others, will present mean tensile stresses in the first place, even before any dynamic load has started to affect the structural elements, and cause *intrinsic mean stress*, or because of other underlying loads affecting it.

This distinction between intrinsic and extrinsic mean stress might appear insignificant, but it is in fact very relevant when considering that *extrinsic* and *intrinsic* mean stresses are governed by different rules and dynamics; the former is related with fast processes and the latter with much slower ones.

Structural elements under tension, for example, tend to be progressively detensioned by relaxation and/or creep, corrosion, or other time dependent and very slow processes that might affect them throughout their service life making them to loose stiffness, even fatigue itself [42]. Hence, a stiffer or tighter struc-

tural element could present higher *intrinsic* mean stress at the very beginning of its service life, after which it will start to be detensioned and it will share its load with other collateral structural elements up to a minimum at the end of its service life. This means that a certain fatigue cycle, due to gusts of wind, for example, will present the same *extrinsic* mean stress, regardless of whether it is during the service life. It will therefore represent a fatigue process, as gusts of wind are a stationary, ergodic process. However, if a certain fatigue cycle occurs before or afterwards then the effects of the *intrinsic* mean stress will not be the same.

3. Mean stress pushing factor

Hence, it is clear that the *total* mean stress affects the fatigue damage of a certain cycle, regardless of its *intrinsic* or *extrinsic* nature. Thus, as most Whöler curves are derived from completely reversed zero mean-stress tests, (i.e. at $\sigma_m = 0$), [8, 11] and as the Palmgren-Miner linear rule states that a certain cycle block, i, damage, D_i, under a constant stress amplitude (or $\Delta\sigma$ range), is the cycle amount in a given block, N_i, divided by the number of cycles until failure, N_f, under block stress range, $D_i = N_i/N_f$, [6, 7], then those cycles until failure, N_f, must be calculated by considering that mean stress. Several methods have been proposed to do so. The most widely used, the Goodman approach [3], see equation (1), appears to be the most accurate when compared to its alternatives from Gerber and Soderberg [4, 5], shown in equations (2) and (3), respectively. Nevertheless, in some cases, like welded steel joints at $\sigma_{max} > \sigma_u/2$, Gerber is more accurate despite being normally too conservative [43]. Besides, in terms of accuracy there are currently other promising proposals, such as the essential work *Nieslony-Böhm* [44]. Among others like modified SWT, as proposed by *Ince-Glinka* [45] or *Karakas* [46] for welding; or like the more accurate modified Walker criterion [47], that is clearly the better one under certain corrosive environments, as pointed out by *Morgantini* [48]. Nonetheless, Goodman is still widely used even as a comparative basis because of a balance

between good accuracy by the safety side and great feasibility.

Thus, the Goodman equation (1) relates the stress range, $\Delta\sigma_{eq}$, of an *equivalent* fatigue cycle at null mean stress ($\sigma_m = 0$) causing the same fatigue damage as the original cycle with its stress range, $\Delta\sigma$, and mean stress, σ_m. In these three equations, σ_u and σ_y are, respectively, the ultimate and the yield stress.

$$\Delta\sigma_{eq} = \frac{\Delta\sigma}{1 - \left(\sigma_m/\sigma_u\right)} \tag{1}$$

$$\Delta\sigma_{eq} = \frac{\Delta\sigma}{1 - \left(\sigma_m/\sigma_u\right)^2} \tag{2}$$

$$\Delta\sigma_{eq} = \frac{\Delta\sigma}{1 - \left(\sigma_m/\sigma_y\right)} \tag{3}$$

Now, the existing mean stress will clearly alter the total number of cycles that a certain structural detail might undergo before failure within the same stress range. The Wöhler curves are derived at a constant mean stress level, typically, of 0 MPa, although it could be higher for a few structural details such as rebars. Some simple procedure is therefore needed to compute the calculations according to the Wöhler curves, while also taking into account the effects of mean stress.

For instance, for a certain number of cycles, N, at a certain stress range, $\Delta\sigma$, and mean stress, σ_m, then the number of cycles to failure, N_0, will be derived from the structural detail characteristic of the Wöhler curve, but at zero mean stress (*0-mean*). So, the apparent *0-mean* damage, D_0, (remember that $\sigma_m \neq 0$) will be computed as the fraction between the number of cycles at such stress level and the number of cycles until failure, see equation (4). This procedure, will in practice neglect the influence of mean stress under fatigue when applied to structural elements with mean stresses other than 0.

$$D_0 = \frac{N}{N_0} \tag{4}$$

In contrast, if the mean stress was anything other than 0, following the same *keep-it-simple* philosophy, previously mentioned in earlier works [49, 50, 51],

based on adaptation coefficients to consider other effects, then the Wöhler curves could be still applied, but only with an equivalent number of cycles, N_{eq}, at null mean stress, $\sigma_m = 0$, and within the same stress range, $\Delta\sigma$.

Then, the *equivalent* fatigue damage D_{eq} done by such equivalent number of cycles N_{eq}, is obtained by the Palmgren-Miner [6, 7] linear rule by simple addition. See equation (5):

$$D_{eq} = \frac{N}{N_{eq}} \tag{5}$$

Therefore, for a certain number, N, of cycles with a certain stress range, $\Delta\sigma$, and a certain mean stress, σ_m, there is a relationship between the fatigue damage estimate when *neglecting* the mean stress, D_0, and when considering it through the *equivalent* damage, D_{eq}, of cycles at $\sigma_m = 0$. This damage amplification due to mean stress can be considered by a *mean stress pushing factor* F_{MSP}, the mathematical definition of which is shown in the following equation (6):

$$D_{eq} = D_0 \cdot F_{MSP} \tag{6}$$

Nevertheless, having the equivalences previously defined by Goodman, Gerber and Soderberg in terms of *equivalent* stress ranges, $\Delta\sigma_{eq}$, the question is why is it useful to consider it through a simple factor? The answer is that some procedures find the fatigue damage under random loadings by neglecting the mean stress. The proposed method can be used afterwards by simple multiplication of the result, block by block, which will be explained in the *case study* section 5.

Thus, the mean stress pushing factor, F_{MSP}, is the quotient of the equivalent damage at zero mean stress and the damage neglecting the mean stress and, substituting equations (4) and (5) into the relationship, yields equation (7):

$$F_{MSP} = \frac{D_{eq}}{D_0} = \frac{N_0}{N_{eq}} \tag{7}$$

Then, Goodman's equation (1) can be converted in the same nomenclature into equation (8):

$$\Delta\sigma_{eq} = \frac{\Delta\sigma_0}{1 - (\sigma_m/\sigma_u)} \tag{8}$$

From that point, equation (8) can be operated into (9), simply by dividing each side by the bare cycle range, neglecting the mean tension, $\Delta\sigma_0$:

$$\frac{\Delta\sigma_{eq}}{\Delta\sigma_0} = \frac{1}{1 - (\sigma_m/\sigma_u)} \tag{9}$$

Now, recalling Basquin's law [18], if the Wöhler curve [8] is placed in a log-log ratio, it can be seen that the number of cycles to failure N_{eq} at an equivalent *0-mean* stress range, $\Delta\sigma_{eq}$, and the cycles to failure at the initial stress range N_0, but simply neglecting the mean stress, $\Delta\sigma_0$, both present a linear relationship with the exponent, m, of the characteristic Wöhler's curve, which turns a plain slope into a log-log ratio. See equation (10):

$$\frac{log(\Delta\sigma_{eq}) - log(\Delta\sigma_0)}{log(N_0) - log(N_{eq})} = \frac{1}{m} \tag{10}$$

So, recalling the property that relates the logarithmic difference with the logarithm of division, equation (10) can be operated upon by substituting equations (7) and (9) into it, yielding equation (11):

$$\frac{log(\Delta\sigma_{eq}/\Delta\sigma_0)}{log(N_0/N_{eq})} = \frac{log\left[\frac{1}{1-(\sigma_m/\sigma_u)}\right]}{log(F_{MSP})} = \frac{1}{m} \tag{11}$$

Finally, from the equation (11), undoing the logarithm leads to the mean stress pushing factor, F_{MSP}: F

$$F_{MSP} = \left[\frac{1}{1 - (\sigma_m/\sigma_u)}\right]^m \tag{12}$$

Consistent with same fatigue theoretical framework and recent alternative approaches [52, 53, 54], this factor can be used with any existing method to derive *only* the fatigue damage within a $\Delta\sigma$ stress range, with the Palmgren-Miner linear accumulation rule, and with the log-log Wöhler curves according

to Basquin's law. Thus, this approach can be used for feasible and safe predictions, but there are other approaches, like *Sutherland-Mandell* [55], combining Goodman at several stress range ratios R with non linear Palmgren-Miner modifications looking for more accuracy at certain cases. The factor to introduce the mean stress effect, σ_m, can be adapted, if the cycle counting method conserves the relevant information in the same way as the Rainflow method. The mean stress effect can also be introduced when it arises from other concomitant *quasi-static* loadings.

4. Three second-order effects of intrinsic mean tension

Nevertheless, it is never enough to consider the mean stress by simply adopting the factor disclosed in equation (12), since the mean stress derived from mean tension induces at least three second-order effects in fatigue. Namely, *cycle quasi-ordering*, *histogram variation*, and second-order *apparent mean tension*. These three second-order effects are disclosed in the following subsections 4.1, 4.2, and 4.3, respectively.

4.1. Cycle Quasi-ordering

Looking at equation (12), it becomes clear that the existence of a concomitant mean tension that induces a corresponding mean stress, σ_m, will suppose an amplification of fatigue damage, D.

A first derivative of that fact is that, when facing a time-dependent variation of that mean tension, then the amplification will also be time dependent, i.e. if $\sigma_m = \sigma_m(t)$ then, accordingly, $F_{MSP} = F_{MSP}(t)$.

A second derivative of that previous fact, when applied to random loadings, generally treated as both *stationary* and *ergodic stochastic* processes, is that if the mean tension, σ_m, tends to decrease with time, then any amplification will also tend to decrease over time. This circumstance is a common occurrence, as when any existing tension in steel beams, rods, cables, tendons, etc. tends to *relax*, then creep and localized plasticity or hole slotting will tend to distribute

stresses around fatigue hot-spots. Besides, a progressively fatigue damaged structural element will tend to lose stiffness, sharing its load with other elements in the same structure that is usually *hyperstatic*. All these factors will contribute to induce a decreasing amplification behavior.

Let us consider, for instance, a stochastic random loading stress, $\sigma(t)$, decomposed into a summation of harmonics, $\sigma(t) = \sum_1^N \left[\frac{\Delta\sigma_i}{2} \cdot (sin(\omega_i \cdot t)\right]$, each with an angular frequency of ω_i and an amplitude of half of the corresponding stress range, $\Delta\sigma_i/2$, depending on the motion energy at each frequency. Then, by the distributive property of the multiplication, an amplification factor, $F_{MSP}(t)$, applied to whole summation is also applied independently to each isolated harmonic. Therefore, for the sake of clarity, the *quasi-order* effect can be shown simply by looking at *one single harmonic*.

Then, we can consider a few stress cycles of a certain isolated harmonic, with a range and an angular frequency of $\Delta\sigma$ and ω, respectively, as defined by equation (13). Purely for demonstrative purposes, if it had a linear decreasing mean stress, σ_m, descending from an initial value, $\sigma_{m,0}$, at an initial time, t_0, to a final value, $\sigma_{m,f}$, at a final time, t_f, then its definition will be reflected by equation (14). Finally, if that mean stress were constant over time rather than time-dependent, and with an equivalent mean value of $\sigma_m = \frac{\sigma_{m,f} - \sigma_{m,0}}{2}$, then it may be defined by equation (15).

$$\sigma\left(t\right) = \frac{\Delta\sigma}{2} \cdot \ sen(\omega \cdot \ t) \tag{13}$$

$$\sigma\left(t\right) + \sigma_m\left(t\right) = \frac{\Delta\sigma}{2} \cdot \ sen(\omega \cdot \ t) + \frac{\sigma_{m,f} - \sigma_{m,0}}{t_f - t_0} \cdot t + \sigma_{m,0} \tag{14}$$

$$\sigma\left(t\right) + \sigma_m = \frac{\Delta\sigma}{2} \cdot \ sen(\omega \cdot \ t) + \frac{\sigma_{m,f} - \sigma_{m,0}}{2} \tag{15}$$

The above equations, (13) to (15), are in fact three different cases: by application of the superposition principle of elasticity, adding 0 or null mean stress in equation (13), a linearly decreasing mean stress in equation (14), and a constant mean stress in equation (15). In Fig 1, the 0-mean stress case, $\sigma_m = 0$,

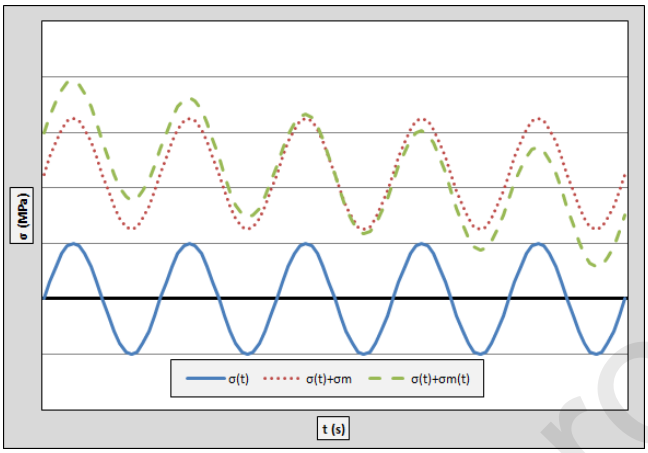

Figure 1: Superposition effect of mean stresses, σ_m, in different cases.

is depicted for a few cycles (blue solid line), as is the linearly decreasing mean stress, $\sigma_m = f(t)$, (green striped line) and, finally, the constant mean stress superposition (red dotted line).

Now, Fig. 2 shows the Rainflow cycle-counting method applied to the case of linearly decreasing mean stress, $\sigma_m = f(t)$, over a few cycles. The first step, depicted in Fig. 2 (green striped lines), is to count half cycles upwards starting at each valley. The second step is to repeat the first step, but looking for half-cycles downwards, starting at each peak, as depicted in Fig. 2 (red dotted line and amber striped-dotted line), the former with the first huge half-cycle from the first peak and the later for the following peaks. It is remarkable that, when neglecting the mean-stress effect, the cycle count identifies the same cycles for the three mean stress cases, with a previous and a single huge cycle covering the mean stress variation for the whole period of study.

Hence, the stress range, $\Delta\sigma$, and the mean tension, σ_m, of each cycle are linearly related, in order to introduce the effect of mean stress, σ_m, depending on the fraction of the period, T, and the mean stress slope or first derivative, $\sigma'_m = \frac{d[\sigma_m(t)]}{dt}$, as shown in Fig. 3.

Finally, it is transformed into its equivalent stress range, $\Delta\sigma_{eq}$, by applying Goodman's equation, (1), to the stress range, $\Delta\sigma$, of each cycle, and the mean

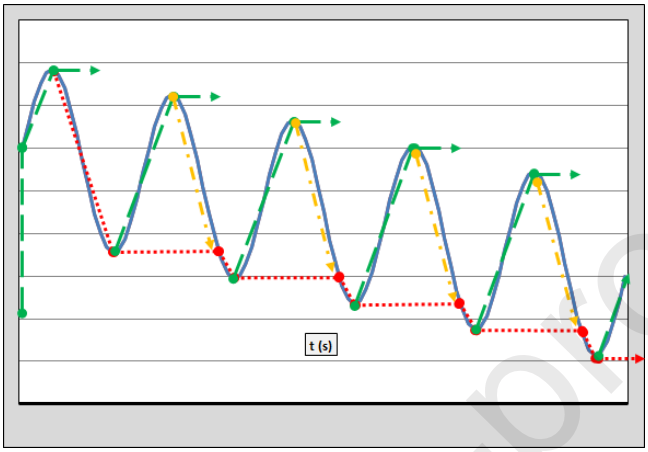

Figure 2: Rainflow cycle count with decreasing mean stress.

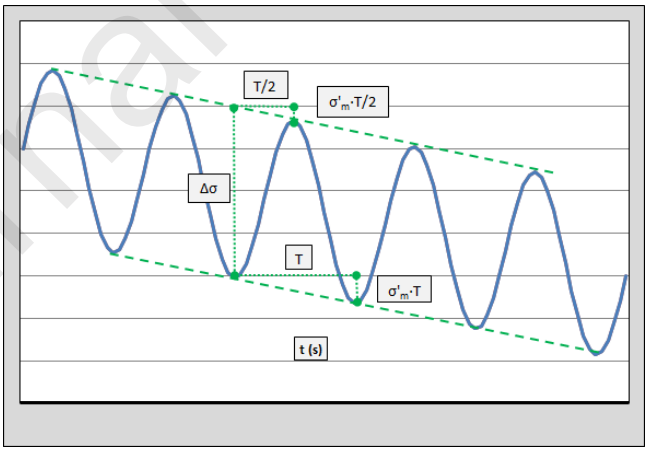

Figure 3: Determination of each cycle's stress range, $\Delta\sigma$, and mean stress, σ_m.

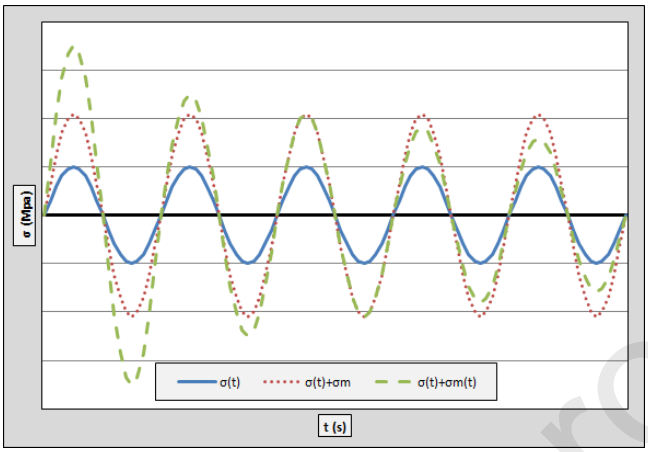

Figure 4: Transformation of each case by Goodman's rule.

stress, σ_m, as depicted in Fig. 4. The 0-mean stress, $\sigma_m = 0$ case, (solid blue line) undergoes no transformation, while the constant mean stress, $\sigma_m \neq f(t) \neq 0$, (dotted red line) undergoes constant amplification of the corresponding peak and valley stress range, $\Delta\sigma$, values, while the linearly decreasing mean stress, $\sigma_m = f(t)$, (striped green line), undergoes a stress range, $\Delta\sigma$, amplification that is higher in former cycles and that progressively decreases. Besides, it remains valid considering aspects like the change in stress ratio $R = \sigma_{max}/\sigma_{min}$ [52, 55, 48, 46, 53, 54], and conservative in pre-strained elements [56].

The question is now whether the above is as a rule generalizable? For instance, for any random loading causing a fatigue process with a concomitant long-term decreasing mean tension, there will be a corresponding slow drop of the mean stress, σ_m, at least when compared to the mean frequency of the process. In such cases, the mean stress function can be discretized into small finite segments of constant slope, where this relationship remains true. Besides, if the random loading is both a stationary and an ergodic process and can be defined as an stochastic harmonic function in the shape of $\sigma(t) = \sum_1^N \left[\frac{\Delta\sigma_i}{2} \cdot (sin(\omega_i \cdot t)\right]$, any amplification factor derived from Goodman's equation (1) and applied simultaneously at any time to all harmonics composing the stochastic process, can be extracted as a common factor of the summation, by a simple distributive

property of multiplication, in the same way as the *mean stress pushing factor*, F_{MSP}.

All of the above implies two things. First, an apparently disordered random loading can produce a *quasi-ordered* fatigue process. Second, mean stress amplification can be derived for a continuous process for some discrete intervals within a certain period. Besides, the total fatigue has to include both the amplification by the F_{MSP} and the sequence effect, that can be achieved by applying the *mean disorder pushing factor*, F_{MDP}, previously presented in [49].

4.2. Histogram variation

Fatigue is a pathology that is mainly, although *not* only studied in metallic structures, where mechanized or threaded details, unions, and abrupt changes of geometry, etc. constitute heterogeneities or discontinuities that affect the mechanical characteristics of the structural detail, making it susceptible to fatigue processes. This type of structure is generally light, constituted by slender elements. In these cases, there are second-order effects, such as *buckling*, that affect the stability of the structures.

In fact, the stiffness of any element under flexural forces and in the presence of axial compression force will apparently decrease, even with the same geometry and inertia, because the deflection of the deformed shape is multiplied by the axial force generating second-order moments that are added to the bending moments, increasing the deformation to the point of equilibrium, if any; an effect that is called *buckling* and that could be the case of compression in beams of lattice girders, pylons, and columns.

However, the same happens in the opposite case when *the axial force is a tension*. In that case, the deflection of the deformed shape is multiplied by any axial tension, giving rise to a negative moment that counteracts the bending. One example might be the deck of an upper arch of a bridge, where the horizontal component of the arch reaction is balanced by the tensility of the deck. The tension therefore assists stability by increasing rigidity.

In view of the above, in cases of *intrinsic* mean tension, and in this type of

slender metallic element, stiffness is highly conditioned by the existence of an axial force of tension or compression. The same is true for natural frequencies and vibrational behavior. So, if the axial force changes, then the rigidity will change as a direct consequence and likewise *the natural frequencies*.

Supposing that the dynamic actions exciting the structure were independent of the internal structural dynamics that vary the axial effort, as in the case of *intrinsic* mean tension, it would mean that the dynamic response would change completely and could even trigger resonance phenomena. Examples could be cables, hangers, braces, etc. with an initial prestressing or tightening that decreases with time, if the length, mass and tension of the cable at a given moment had a frequency coupled with incident wind speed, imposed vibrations, and so on.

One way of mitigating this possible effect would, first of all, be to find the *input* power spectrum *PSD*, $S_x(f)$, and then the frequency response function *FRF*, $|H(f)|$, depending on the maximum and minimum tension of the process. If any of the peaks of both functions matched each other, the maximum *output* power spectrum, $S_y(f)$, could be obtained as the product of both factors. In the intermediate situations, despite conservative estimates with a safety margin, the tension maximizing the response or *output* PSD, $S_y(f)$, will be chosen. See Fig. 5.

Hence, it is a question of identifying the predominant input frequencies with greater energy in the incident action and any coincident frequencies. In that case, the first strategy would be to avoid natural frequencies coinciding with these frequencies, either by designing the tension of the concrete elements, perhaps with stratified strategies, or by simply taking into account the worst situation in the calculation and verifying compliance against fatigue.

For instance, the case of a bi-supported, 6 m length, *square hollow section* SHS 100.5 profile is presented, in order to illustrate that effect. In addition to its own weight, it is loaded with 300 kg of uniformly distributed dead load. This profile has a decreasing tension from 100 to 0 kN and it is proposed to determine the *natural frequencies* as a function of the aforementioned tension. For the sake

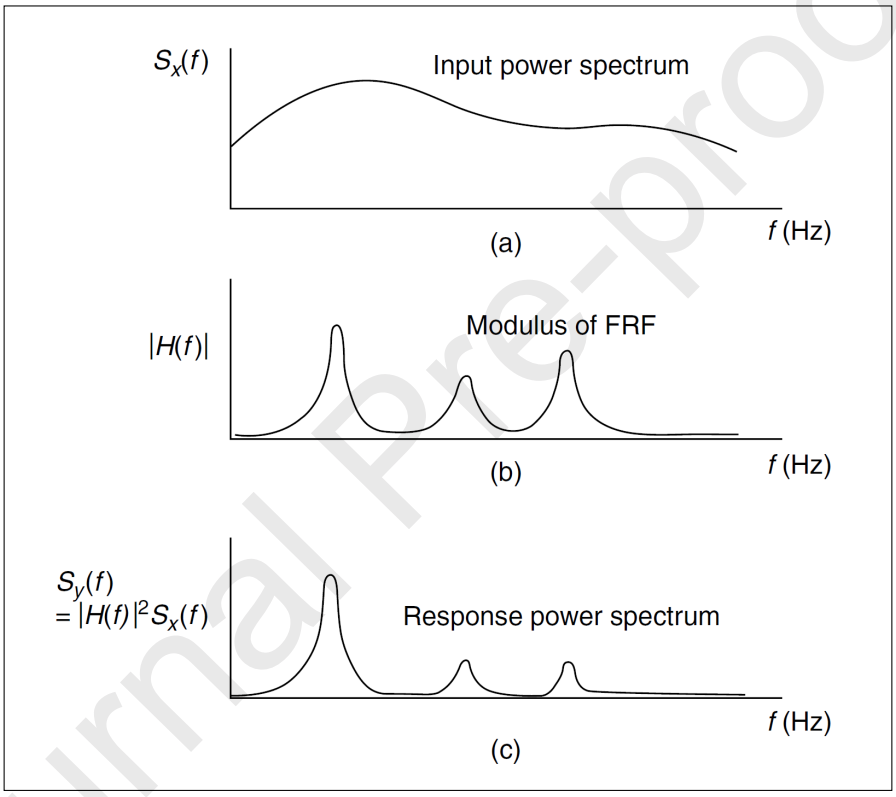

Figure 5: Derivation of response power spectra.

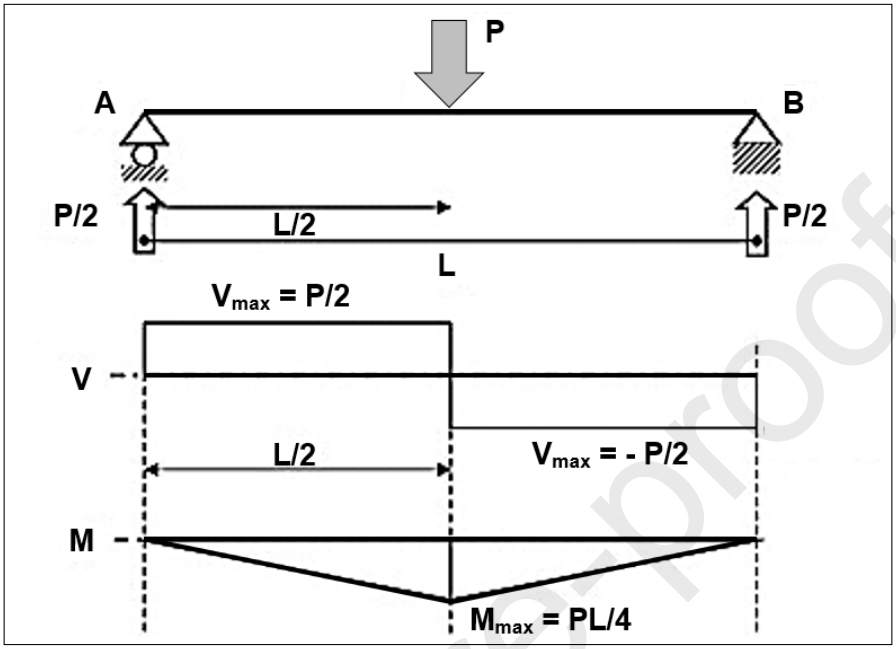

Figure 6: Bi-supported beam model.

of simplicity, an equivalent Single Degree of Freedom (SDOF) model is applied. An MDOF case is presented in the case study section 5.

So, the first step is to determine the deflection caused by 1 kN at span center in a conventional bi-hinged model, such as the one shown in Fig. 6, following the *virtual works* method.

In the case of a beam without tension, the deflection law is derived from the equation of elasticity (16), as a function of the x coordinate, as expressed in equation (17), for the domain of $0 \leq x \leq L/2$, and the value of that equation is shown in equation (18) at span center:

$$y''(x) = -\frac{M(x)}{E \cdot I} \tag{16}$$

$$y(x) = -\frac{P \cdot x^3}{12 \cdot E \cdot I} + \frac{P \cdot L^2 \cdot x}{16 \cdot E \cdot I} \tag{17}$$

$$y(L/2) = \frac{P \cdot L^3}{48 \cdot E \cdot I} \tag{18}$$

In the case of an axial load under tension, N, the differential equation to obtain the deflection law, $y(x)$, is (19). By substituting (20), we arrive at equation (21), which will have to be solved:

$$y'' - \frac{N}{EI} \cdot \ y = -\frac{1}{2} \cdot \frac{P}{EI} \cdot \ x \tag{19}$$

$$\alpha^2 = \frac{N}{EI} \tag{20}$$

$$y'' - \alpha^2 \cdot \ y = -\frac{1}{2} \cdot \frac{P}{EI} \cdot \ x \tag{21}$$

Then, after decomposing the differential equation problem into an homogeneous part, y_{GH}, plus a particular solution, y_{PC}, a general solution to the homogeneous part is equation (22), while the particular solution of the complete equation is in the form shown by equation (23). So, (24) represents a summation and the general solution of the complete y_{GC} is shown below in equation (25):

$$y_{GH} = C_1 \cdot \ e^{\alpha x} + C_2 \cdot \ e^{-\alpha x} \tag{22}$$

$$y_{PC} = \frac{P}{2N} \cdot \ x \tag{23}$$

$$y_{GC} = y_{GH} + y_{PC} \tag{24}$$

$$y_{GC} = C_1 \cdot \ e^{\alpha x} + C_2 \cdot \ e^{-\alpha x} + \frac{P}{2N} \cdot \ x \tag{25}$$

For instance, it is sufficient to impose the boundary conditions, shown in (26), in order to find the constants, C_1 and C_2. Then, deriving the values of the

constants, as shown in the following equations (27) and (28), and substituting them into equation (25) above, will yield equation (29) that is shown below:

$$y(0) = 0 \wedge \ y'(L/2) = 0 \tag{26}$$

$$C_1 = -\frac{P}{2N} \cdot \frac{1}{\alpha \cdot (e^{\alpha \cdot L/2} + e^{-\alpha \cdot L/2})} \tag{27}$$

$$C_2 = \frac{P}{2N} \cdot \frac{1}{\alpha \cdot (e^{\alpha \cdot L/2} + e^{-\alpha \cdot L/2})} \tag{28}$$

$$y(x) = \frac{P}{2N} \cdot \left[\frac{e^{-\alpha x} - e^{\alpha x}}{\alpha \cdot (e^{\alpha \cdot L/2} + e^{-\alpha \cdot L/2})} + x \right] \tag{29}$$

It can now be seen in Fig. 7 that the lower the the tension, then the closer are the values of derived equation (29) to those of equation (17).

Fig. 7 shows the deflection value at several x positions for the case of a load $P = 1 \cdot kN$, located at span center and at $N = 0 \cdot kN$ and at $N = 100 \cdot kN$ of tension load; a substantial change in the deflection value, in the form of increased stiffness, can be seen.

Thus, the values of the natural frequencies, in Hz, for a *Single Degree Of Freedom* SDOF bi-supported beam model, are listed in the last column of Table 1, related to the last row as a function of the tension load, *N*, shown in the first column. The other columns showing the flexibility v derived from beam deflection, the stiffness k as the inverse of flexibility, the beam stiffness to mass ratio k/m, and the corresponding SDOF angular and simple frequencies, ω and *f*. Accordingly, as can be seen, in a long process that is sustained over time, while the tension starts at 100 kN and is then reduced, due either to relaxation or other processes, to 0 kN, the natural frequency varies between 3.72 and 2.94 Hz, see Fig. 8. This frequency change after loosing stiffness by detensioning is consistent with recent studies, such as *Wu et Al.* [42].

One consequence is that, if the incident dynamic action, treated as stationary, has a frequency of 3.5 Hz due to external causes, such as wind buffeting

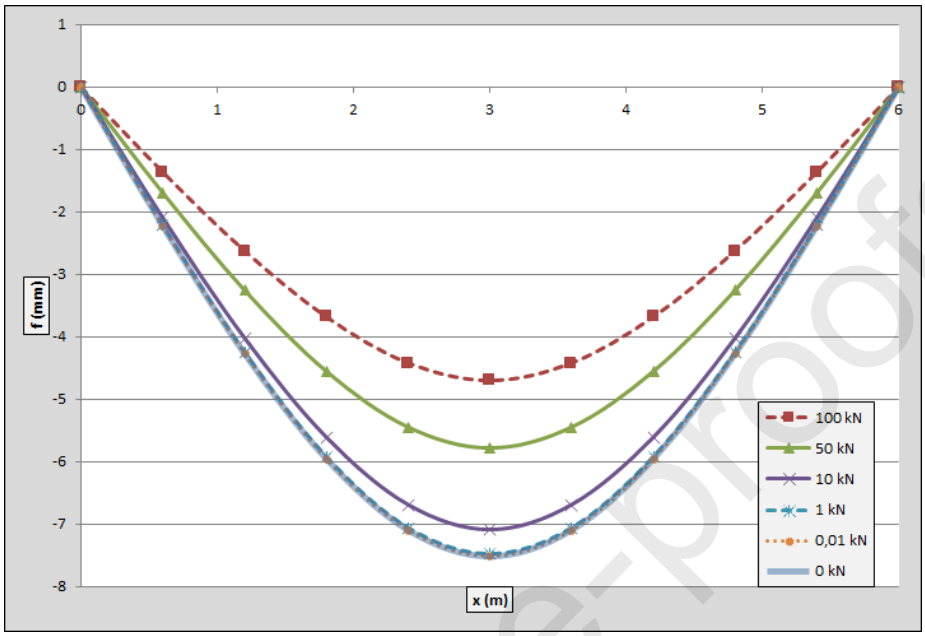

Figure 7: Deflection law $y(x)$ in mm.

given the rugosity of the windward terrain, or traffic, or a pedestrian promenade area, etc. ., and if the calculation of the response power spectra, $S_y(f)$, were under the initial or final tension conditions, then the response would spuriously be diminished, since the real fact is that the *resonant response* would be much more harmful and *will certainly occur* at a certain moment of the service life of the element.

Three corrections are therefore needed for the situation described above to be applicable to a certain case study:

1. Calculate the response power spectra, $S_y(f)$, in the worst scenario, i.e. the one where the natural frequencies of the FRF functions, $H(f)$, are coincident with the dominant frequencies of the input power spectra, $S_x(f)$. For instance, in the present case, it would be for tension loads of around 70 kN. For a more complete analysis, the service life could be discretized into several sub-periods, with several tension load hypotheses and their corresponding frequencies.

Table 1: SDOF natural frequencies, f [Hz], depending on tension load, N [kN].

N	**v**	**k**	**k/m**	ω	**f**
[kN]	**[mm/kN]**	**[kN/mm]**	**[(rad/s)²]**	**[rad/s]**	**[Hz]**
0	7.52	0.13	342.08	18.50	2.94
10	7.09	0.14	362.64	19.04	3.03
20	6.71	0.15	383.17	19.57	3.12
30	6.37	0.16	403.68	20.09	3.20
40	6.06	0.16	424.15	20.59	3.28
50	5.78	0.17	444.60	21.09	3.36
60	5.53	0.18	465.02	21.56	3.43
70	5.30	0.19	485.42	22.03	3.51
80	5.09	0.20	505.79	22.49	3.58
90	4.89	0.20	526.14	22.94	3.65
100	4.71	0.21	546.46	23.38	3.72

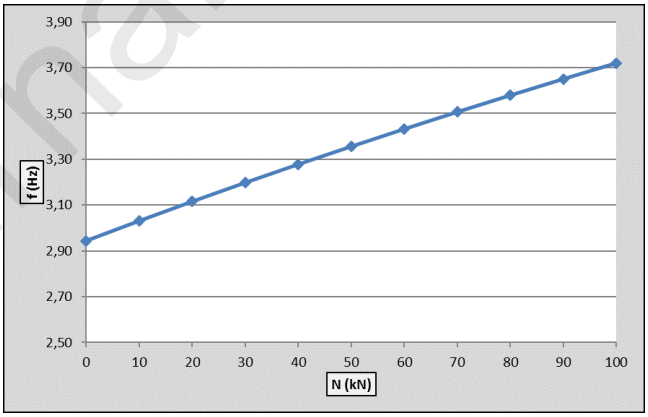

Figure 8: Natural SDOF frequency depending on axial load f=f(N) in Hz.

2. Consider the *quasi-order* due to detensioning, considering the full range of both maximum and minimum loads. In the present case, from 100 kN to 0 kN.
3. Correct the average stress with the Goodman's equation or the derived mean tension pushing factor, F_{MTP}, considering the average tension caused by the higher tension of the following: the one giving the maximum response power spectrum, $S_y(f)$, and the process mean value, $(N_{max} + N_{min})/2$; in the present case, 70 kN.

4.3. Second-order apparent mean tension

The way that mean tension can generate second-order effects that alter the histogram has been described in the previous section. In this section, the same idea is expressed *in reverse*, drawing attention to how second-order effects such as buckling can cause induced medium tensions, which are not extrinsic, because they are not due to the action itself, nor essentially intrinsic, as they are not part of the element itself, but are intrinsic to the whole structural system.

Indeed, if a constant action is maintained in the structural system, when a structural element is unloaded, then the structure seeks to maintain equilibrium, by a redistribution of its load among its constituent elements, causing increased mean tension among the others. This unloading, if due to effects such as the buckling of slender elements under compression, could induce different types of stiffness in the element, when induced by either compression or traction. So if a dynamic action is applied to the element with a completely reversed cycle, its load will be higher during the part of the cycle under tension and lower during the part of the cycle under compression, causing an effective *apparent mean tension* in the cycle.

A clear example of this phenomenon would be the bracing frames of buildings that withstand the horizontal actions of wind and seismic activity by means of axial truss-like elements: i.e. the *Concentrically Braced Frame* CBF systems. Fig. 9 presents the most common typologies shown in Eurocode 8 [57], as stated in [58].

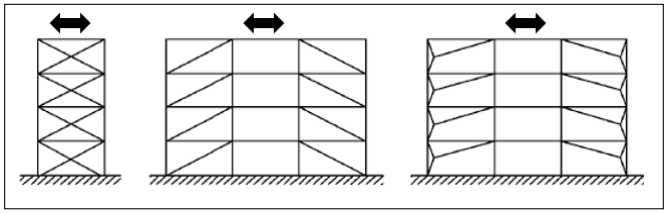

Figure 9: CBF bracing typologies to withstand lateral loading of buildings, as per Eurocode 8.

In those CBF systems, only the contribution of the tensioned diagonal braces is considered, Art. 6.3.1 (3) [57], completely neglecting the contributions of the diagonal braces under compression. It is not that they have no *de facto* collaboration, but the buckling reduces the effectiveness of any compression effort. Any consideration of that effort will, therefore, be conservative.

By imagining a completely reversed horizontal dynamic action, in an idealized structure with no imperfections, the system will be antimetric and, at any one time, the tensile stress of a diagonal brace will be equal, in module, to the compressive stress of the other. Nevertheless, in reality, imperfections cause the diagonal braces to buckle under compression and, in order to rebalance the system, all the compression that one diagonal brace is not providing will be converted into tension in the other. When the cycle changes and the diagonal brace previously under tension is under compression, it will begin to buckle, losing compression and causing tension overload in the other diagonal brace previously under compression.

Thus, if by an alternate action, at one extreme of the cycle, two idealized X-bracing diagonals were correspondingly loaded at 100 kN tension first and -100 kN compression, at the other extreme of the cycle they would logically be loaded at -100 kN and 100 kN, respectively, completing totally reversed cycles with a mean load of 0 kN and an amplitude of 100 kN. Nevertheless, the diagonal braces are never ideal in reality and the brace under compression at one extreme of the cycle will actually lose effort, with compression for example of up to -50 kN, which will overload the other diagonal brace under tension by

up to 150 kN, a situation that is reversed at the other cycle extreme. Hence, the diagonal would be initially tensioned at 150 kN and then compressed up to -50 kN compression. Therefore, in reality, despite the external reversed action, applied with 0-mean tension, in practice it causes cycles from -50 kN to 150 kN, with a mean tension of 50 kN and an amplitude of 100 kN, which is precisely the *second-order apparent mean tension*.

Such an effect needs always to be considered, through the application of the appropriate mean tension correction coefficients F_{MSP}, derived from Goodman, Gerber or Soderberg, as previously mentioned.

5. Case study

We will consider a 12-storey building with 8 planes of shearing bracing, made of X-type diagonals, 4 of which face each horizontal direction forces, x and y, with a length in plan view of 36 m, a width of 24 m and, finally, a height of 37.2 m. The storey dimensions are regular, with a height of 3.1 m and a span between columns of 6 m, and a total effective mass at each storey of *151,200 kg*. See Fig. 10.

The building faces wind loading, with a basic velocity of *29 m/s* and a terrain category II, according to Eurocode 1 [24, 59], defining the terrain roughness for wind loading. Thus, under such conditions, the axial loading at the bottom storey, due to wind loading in the ultimate limit state is 291,85 kN, while the diagonal bracing profiles are *UPN-100*, the columns are HEB-180 profiles, and the crossbeams are HEB profiles, all made of S-275 steel [9]. The diagonal bracing connections are *6x M12 10.9 steel bolts*, which attach the diagonal braces to a gusset plate welded at the HEB profile corner [10].

At the time it was built, the shearing plane was executed by building the columns and crossbars first, completing the gantry, welding the gusset plates to each corner, and then attaching the diagonal braces. Nevertheless, when placing the diagonal braces, their temperature was slightly higher than the gantry, but only by *10 °C*. This difference might not seem very much, although when

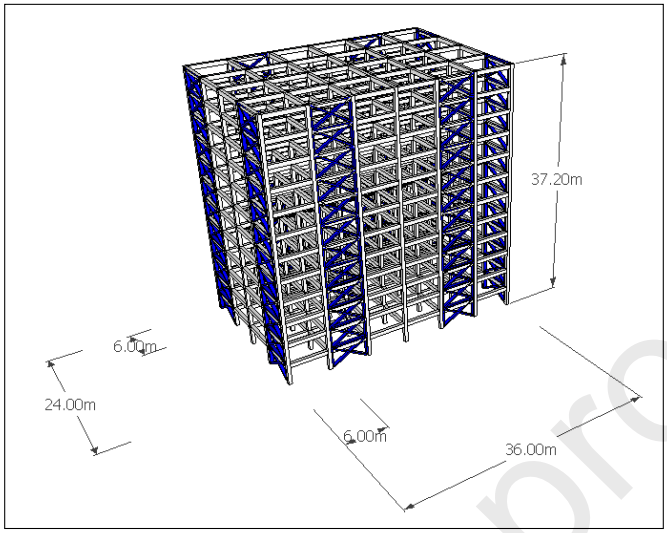

Figure 10: Geometry of the building for the case study.

placing the braces and fixing the connections, the temperature tended towards equilibrium, so the diagonal braces tended to shorten, causing an equivalent mean tension. Note that a difference of 10 degrees is quite common for on-site works where completion can take several days. Nevertheless, even though this tension is unintentional in this case study, the diagonal bracing normally has a degree of pretensioning for proper performance. In this case, the temperature increment is equivalent to a pretensioning of 34.04 kN.

Hence, two models are produced to represent a shearing plane under two hypothetical situations. A first one where the diagonal braces remain under tension, due to the temperature increment, $\Delta T = 10^{\circ}\ C$, in the execution phase, and a second situation when it loses its initial tension after several cycles and progressive hole slotting at bolt connections. In those models, the diagonal braces are considered as non-linear elements, working only under tension and in no case under compression, with corresponding temperature gradients depending on the situation.

These models where then used to represent an equivalent lumped mass, Multi-Degree Of Freedom *MDOF*, system, considering horizontal motion at

each storey at a total of 12 modes. A three-way $12x12$ matrix was required, corresponding to mass, damping and stiffness matrix, to represent the system. The mass matrix was a diagonal matrix, with a storey mass at each diagonal element. The damping matrix is another diagonal matrix, with the damping at each storey, that can be considered almost but not completely regular and equivalent to a conservative figure of 2% damping. Finally, the stiffness matrix was the inverse of the flexibility matrix that was slightly more complicated.

A force of $F = 100kN$ was introduced at each storey in the model to obtain the flexibility matrix, registering the consequent displacements at each storey, but one force at a time, filling the 12×12 flexibility matrix f, in both situations. The stiffness matrix was therefore the inverse of the flexibility matrix. There was no need to reproduce the full matrix of both situations, but it was sufficient to show the stiffness increment, when the load was applied to the uppermost storey with diagonal bracing under tension. The consequent horizontal displacement at the uppermost storey was 102 mm, while it grew to 112.9 mm when applied without any load, implying a drop in stiffness.

Then, the *eigenvalues* and *eigenvectors* of the flexibility matrix were found and the corresponding *frequency response functions FRF* of each mode i, $H_i(f)$, were developed, to obtain the natural frequencies and the natural modes of vibration. Thus, with the FRFs, the frequency response function of the motion at the first storey, z_1, caused by the force at each storey, i, was then derived by $H_{z1Fi}(f)$.

For instance, in the following Fig. 11, the frequency response function of the motion at the first storey is shown due to wind buffeting at the 12^{th} storey with tensioned and detensioned diagonal bracing.

The solid blue line represents the situation where the equivalent *intrinsic* tension corresponds to $\Delta T = 10^{\circ}\ C$, while the red striped line shows the situation where any initial tension is lost. In reflection, it can be seen that this approach is not only about considering the mean stress through Paris' law, or as it is considered in Goodman, Gerber and Soderberg, as it changes the structural response itself, varying the natural frequencies, in consistency with *Wu et Al.* at

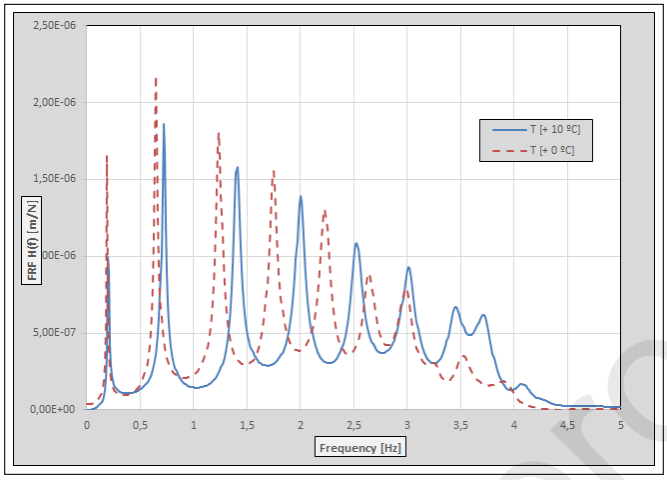

Figure 11: Frequency response function of motion at the first storey, due to wind buffeting at the 12^{th} storey with tensioned and detensioned diagonal bracing.

[42] when loosing stiffness. Hardly significant under a broad band uniform processes, it is in narrow banded ones, if a peak at the input PSD could match the peak at the FRF during the detensioning process, because at this point it could develop resonance effects and very damaging fatigue. In this case, the natural frequencies tend to decrease, but their peaks become higher. One explanation could be the non-linearity, if the diagonal braces are only working under tension, or only under compression, because they need to surpass the pretension before buckling, which is relevant in terms of stiffness and effective damping elements.

The wind load spectra were estimated with the method proposed by Davenport [60], which is widely used. As this is an external force, the *extrinsic* process applies to both situations. Accordingly, in Fig. 12 the normalized wind spectra (a), scaled to disregard mean wind velocity and frequency, is depicted and the PSD of the wind loading force at the first, the sixth, and the twelfth storeys (b).

The power spectral density of the displacements at the first storey, caused by the wind loading at each storey can therefore be derived, see Fig. 13. Besides, the power spectral density of the stress at the joining bolts is directly derived

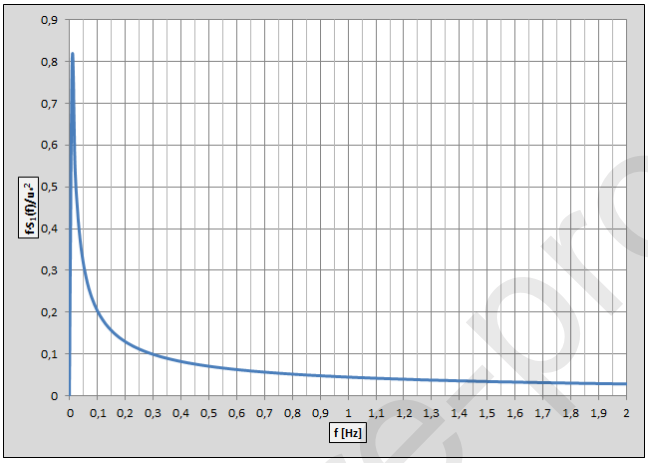

(a) Davenport's normalized wind spectra.

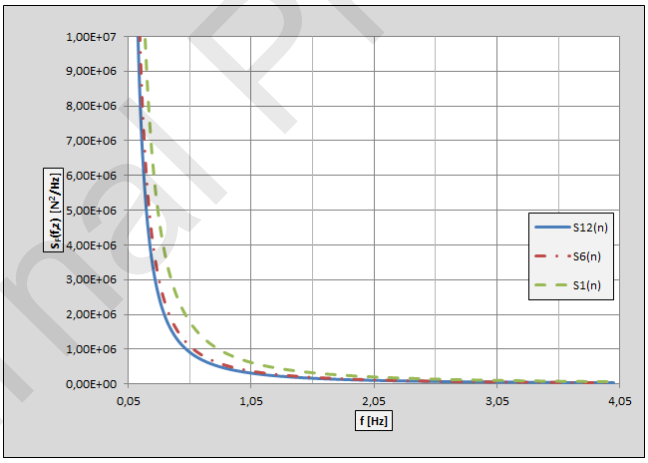

(b) Power spectral density of wind loading force.

Figure 12: Wind loading spectra.

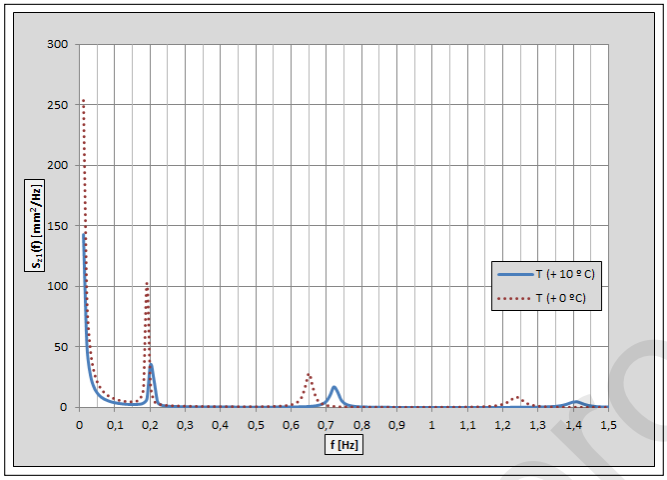

Figure 13: PSD of the displacements at the first storey due to wind buffeting the whole building.

from the displacement measurements, considering the relationship between displacement and axial load, and the relationship between axial load and stress at the bolts, considering their effective resistant sections.

In both cases, the solid blue line depicts the spectra with tensioned diagonal bracing, while the red dotted line depicts the scenario of the detensioned diagonal bracing. The power spectral density of the stress at the bolts is the required PSD.

5.1. Cycle account and fatigue damage

There are several methods applied to cycle counting starting with a wide-band stress spectra in random loading, such as the methods proposed by Zhao-Baker [61], Petrucci-Zuccarello [62], $\alpha_7 5$ [63], the very promising Tovo-Benasciutti [37, 35, 36], well fitted for broad-band Gaussian and non-Gaussian processes, as pointed out by Ding and Chen [64], and Dirlik [65], along with recent improvements to consider somehow the mean stress effect [52, 53, 54]. Finally, there are recent interesting proposals too, like the *bands* method by Braccesi et Al. [66], dividing the broad band PSD in frequency bands, applying Rayleigh distribution [67, 68] at each band, and finally combining all damage.

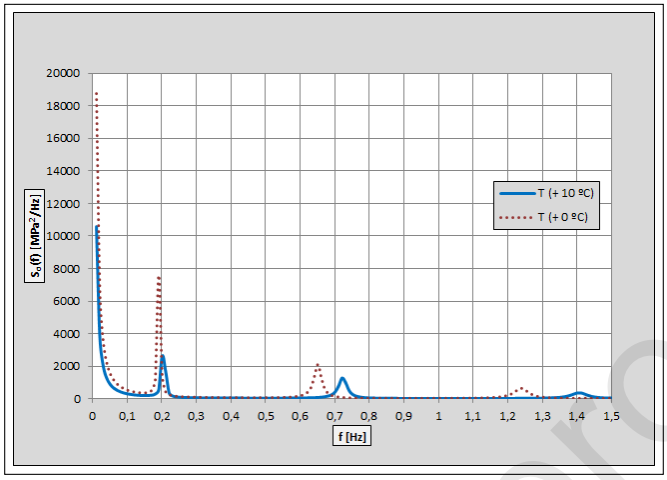

Figure 14: PSD of the bolt stress at the first storey caused by the wind over the whole building.

Dirlik method will be used for this case study, as it is still regarded as the most accurate [69, 70, 71], but others could be applied. In fact, depending on the case, a recent comparison by Mrsnik [38] set Tovo-Benasciutti and Zhao-Baker as the preferred methods after Dirlik.

Following this procedure, based on the PSD moments, the expected peaks per second were 1.49 and 1.44, respectively, with tensioned and detensioned diagonals, and the expected 0-stress crossings, were 0.73 and 0.7, likewise respectively. This difference might not appear very large, but it becomes clearer when deriving the range probability and histogram variation. See Fig. 15 and Fig. 16, respectively. In the interests of clarity, the cycle amount is calculated for a single year of the service life, considering total seconds, one cycle per peak, and peaks per second.

The first thing brought to our attention is the second-order effect of an intrinsic mean tension in the histogram variation, already mentioned in subsection 4.2. Among other things, such variation implies a further modification of *Nieslony-Böhm* [52, 53, 54] if adapting the PSD before applying a rainflow cycle distribution mehod such as *Dirlik*. The second issue is that, when barely applying the Palmgren-Miner rule, considering a detail category of 100 MPa at

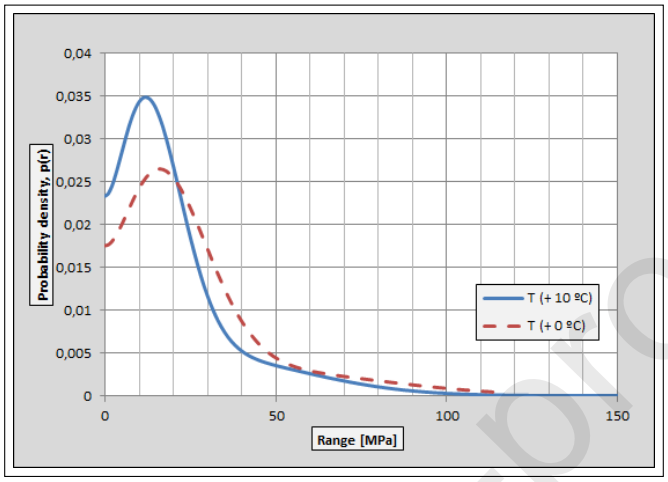

Figure 15: Probability density of cycle ranges according to Dirlik's method with tensioned and detensioned diagonal bracing.

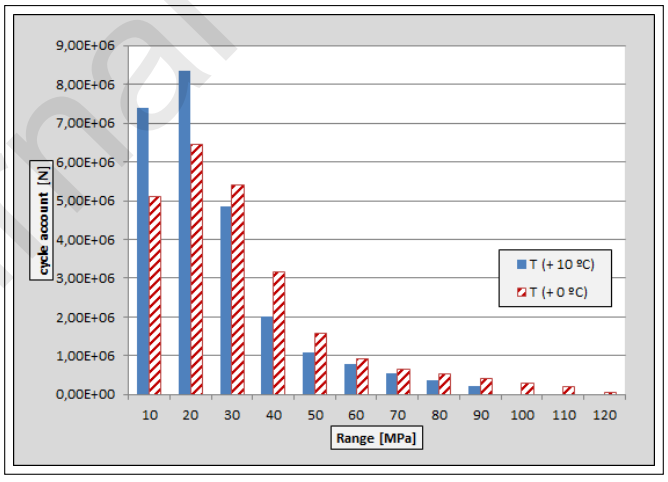

Figure 16: Cycle histogram by Dirlik method with tensioned and detensioned diagonal bracing.

Table 2: Fatigue Damage with detensioned diagonals.

$\Delta\sigma$	ni	Ni	Di
10	7.40E+06	2E+11	0.00%
20	8.35E+06	6.24E+09	0.13%
30	4.85E+06	8.21E+08	0.59%
40	2024607	1.95E+08	1.04%
50	1097274	6.38E+07	1.72%
60	788249	2.57E+07	3.07%
70	555819	1.19E+07	4.68%
80	3.55E+05	6.09E+06	5.83%
90	2.05E+05	3.38E+06	6.07%

$2 \cdot 10^6$ cycles according to Eurocode 3, then the fatigue damage is *23.1%* with tensioned diagonal bracing and *49.1%* with detensioned bracing. See Tables 2 and 3.

However, the tension range of each cycle was not taken into account in Dirlik's method, since the element is unable to withstand compression forces because of buckling. Mean stress must therefore be considered, through the mean stress pushing factor previously defined in equation (12). In the first scenario, a temperature increment, $\Delta T = 10°C$, leads to a mean tension of $T = 34.02kN$ at the diagonal brace, causing a mean stress at each bolt of 67.5 MPa, each with a resistant section of $84mm^2$. Besides, on the safety side, each range, $\Delta\sigma$, is considered to start from that stress level, meaning an apparent mean stress of half the cycle range. Accordingly, Table 4 discloses the corresponding numerical results.

In the second scenario, the detensioned diagonal braces presented no *intrinsic* mean stress. Nevertheless, the non-linearity caused by compressed diagonal buckling led to an *apparent mean stress* of half the stress range, as it only works under tension. Accordingly, Table 5 discloses the corresponding numerical results..

Table 3: Fatigue damage with detensioned diagonals.

$\Delta\sigma$	ni	Ni	Di
10	5.10E+06	2E+11	0.00%
20	6.44E+06	6.24E+09	0.10%
30	5.40E+06	8.21E+08	0.66%
40	3161782	1.95E+08	1.62%
50	1580030	6.38E+07	2.47%
60	907748	2.57E+07	3.54%
70	662495	1.19E+07	5.58%
80	5.24E+05	6.09E+06	8.60%
90	4.02E+05	3.38E+06	11.90%
100	2.92E+05	2.00E+06	14.63%
110	2.00E+05	1.24E+06	16.13%
120	6.40E+04	8.02E+05	7.98%

Table 4: Fatigue damage considering *intrinsic* and *apparent* mean stress with tensioned diagonal bracing.

$\Delta\sigma$	n_i	N_i	D_i	σ_m	F_{MSP}	$D_{eq.i}$
10	7.40E+06	2E+11	0.00%	72.5	1.46	0.01%
20	8.35E+06	6.24E+09	0.13%	77.5	1.50	0.20%
30	4.85E+06	8.21E+08	0.59%	82.5	1.54	0.91%
40	2024607	1.95E+08	1.04%	87.5	1.58	1.64%
50	1097274	6.38E+07	1.72%	92.5	1.62	2.79%
60	788249	2.57E+07	3.07%	97.5	1.67	5.13%
70	555819	1.19E+07	4.68%	102.5	1.72	8.04%
80	3.55E+05	6.09E+06	5.83%	107.5	1.77	10.30%
90	2.05E+05	3.38E+06	6.07%	112.5	1.82	11.02%

Table 5: Fatigue Damage considering *intrinsic* and *apparent* mean stress with detensioned diagonal bracing.

$\Delta\sigma$	n_i	N_i	D_i	σ_m	F_{MSP}	$D_{eq.i}$
10	5,10E+06	2E+11	0,00%	5	1,03	0,00%
20	6,44E+06	6,24E+09	0,10%	10	1,05	0,11%
30	5,40E+06	8,21E+08	0,66%	15	1,08	0,71%
40	3161782	1,95E+08	1,62%	20	1,11	1,80%
50	1580030	6,38E+07	2,47%	25	1,13	2,81%
60	907748	2,57E+07	3,54%	30	1,16	4,12%
70	662495	1,19E+07	5,58%	35	1,19	6,67%
80	5,24E+05	6,09E+06	8,60%	40	1,23	10,55%
90	4,02E+05	3,38E+06	11,90%	45	1,26	14,98%
100	2,92E+05	2,00E+06	14,63%	50	1,29	18,91%
110	2,00E+05	1,24E+06	16,13%	55	1,33	21,40%
120	6,40E+04	8,02E+05	7,98%	60	1,36	10,87%

Thus, consideration of the mean stress value will raise the fatigue damage from 49.91% up to 92.9%, in the case of detensioned diagonal bracing, and from 23.1% to 40.05%, in the case of tensioned diagonal bracing. Its consideration is therefore not optional, as the fatigue damage that is forecast will otherwise lead to unsafe predictions.

Finally, cycle *quasi-ordering* needs to be considered as the mean induced order. For the tensioned diagonal bracing, the average cycle, calculated as simple weighted average in the corresponding histogram has an average stress range of 25.58 MPa and an average mean stress of 80.29 MPa, meaning an equivalent stress range of 27.81 MPa at 0 mean stress in accordance with Goodman's equation application (1). The average stress range of 31.74 MPa and the average mean stress of 15.87 MPa, for the detensioned diagonal bracing, implies an equivalent stress range of 32.25 MPa. The sequence effect coefficient proposed in [49] should be applied for its consideration. In this case it was negligible with a mean stress range decrease of only 5 MPa.

As a final clarification, the three mentioned *second-order* fatigue effects are not specific for this case studied. Cables, say-cables, superior arch bridge decks, braces, hangers, rods, beams under tension (within a truss or a framed tube building), a curtain wall, pre-tightened bolts, tendons and the like are susceptible to such effects. Generally speaking, anything under tension could experiment *cycle quasi-order* and *histogram variation* if gradually losing tension and stiffness accordingly. Besides, at any system supported by a plurality of elements (e.g. beams), when one of them start to loss stiffness, it is translated in a load sharing rearrangement within the others, causing *apparent mean stress* on them.

6. Discussion

The proposed procedure is well suited for structural details belonging to large infrastructures such as buildings, bridges, industrial facilities, towers, reservoirs, aerogenerators and the like, executed on-site and subjected to random loadings such as wind, traffic or low seismicity. Under these scenarios dealing with un-

certainty, the added value of a prediction lies in the balance between safety, actual material saves and cost effectiveness of the analysis. Accordingly, it is an evolved procedure based on the correction of frequency domain calculation, application of Dirlik's [65] (or equivalent) method to deduce Rainflow cycle histograms [26] and fatigue damage calculation, to consider *extrinsic* and *intrinsic* mean stresses and its derived *second-order fatigue* effects.

The case study revealed that, in some cases, the change in an intrinsic mean tension could lead to a change in the global system stiffness, changing the cycle histogram. In the case presented in the previous section, a tension due to a common difference of temperature left a difference in fatigue damage according to the plain Palmgren-Miner linear rule application of *23.1% to 49.1%*. Therefore, an extrinsic mean stress could lead to different ranges but an intrinsic mean stress could lead to completely different fatigue loading. The way to deal with these differences is to discretize the linear process of detensioning, by considering a half period with tensioned diagonal bracing and a half period with detensioned ones, which would yield predicted fatigue damage of 36.1%.

There again, the non-linearity caused by buckling of the diagonal bracing leads to apparent mean tensions of 45 and as much as 60 MPa in the cases of tensioned and detensioned diagonal bracing, respectively. This apparent mean tension, in isolation, caused a pushing factor of 1.36 under detensioned diagonal bracing scenarios, while added to existing intrinsic mean stress lead to a mean stress pushing factor of up to 1.82, increasing fatigue damage substantially, which yielded an average fatigue damage of 66.48 kN.

The sequence effect was calculated in this case, following the rule already disclosed in [49], considering the mean cycles from an average range of 27.81 MPa to 32.25 MPa. However, it was negligible in this case. For instance, the ultimate stress of a 10.9 steel bolt was 1000 MPa, so the equivalence in accordance with Goodman's ratio would be very much lower than in most cases for common structural details made of carbon steel.

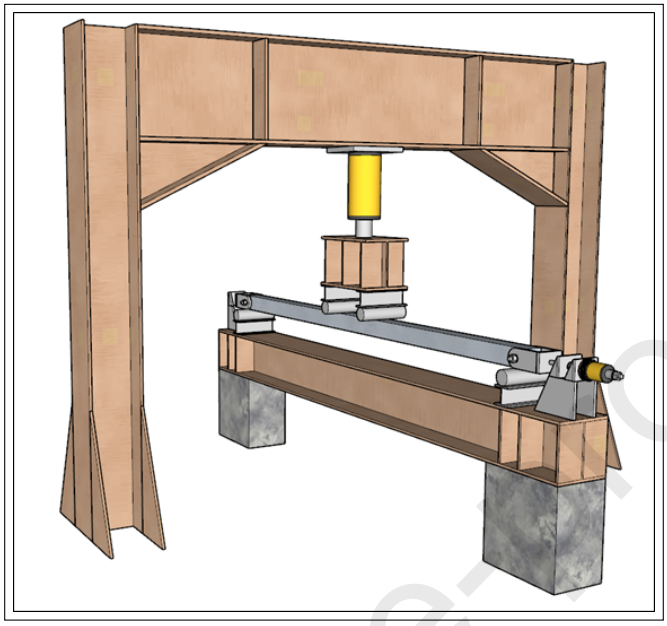

Figure 17: SDOF testing system including variable intrinsic mean stress.

7. Future works

Now, once the theoretical framework has been developed on the basis of the partial experimental evidences and previous works in literature, it is time to define at least the *minimum experimental setup* to research on the importance of such *second-order fatigue effects*. Indeed, the case study was developed in two situations with tensioned and detensioned diagonals, but the reality will be divided in several intermediate situations. This could lead, in one hand, to some intrinsic mean stress at whose frequency the sample starts to develop resonance, with very damaging effects to fatigue, meaning this *before and after* procedure underestimated the consequences. While, on the other hand, this intermediate resonance could lead to *cycle quasi-ordering* only from a certain stage to the end. Accordingly, the experimental setup shown in Fig. 17 discloses a *SDOF* testing system able to test a beam sample analogous to the one proposed in section 4.2. It is based on a rail fatigue test with an hydraulic pulsator imposing a variable force to a beam, but with a system able to tension it.

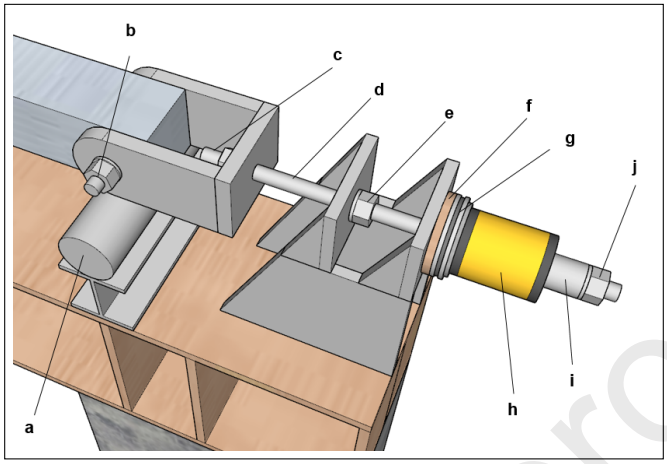

Figure 18: Cycle histogram by Dirlik method with tensioned and detensioned diagonal bracing.

The system to add variable intrinsic mean stress to the beam sample is divided in a passive and an active extreme. The next Fig. 18 shows in detail the active zone, while the passive is similar but up to the locking nut and washer. The active extreme is composed of a support a, to provide a vertical reaction, with a pin b attaching a hinged grip system. Then, with the anchoring nut and washer set c at one end of the threaded rod d, it is possible to transmit tension to the sample simply by pulling such rod d. In order to do it, at the other end of the threaded rod d, there is a set composed by a fixing nut and washer set j, that is pushed by the inner cylinder i of an hydraulic press h, whose reaction passes by the pressure plate g and the supporting disk f to a passive support. Finally, the last feature is the locking nut and washer e that enables the possibility to maintain a certain level of tension during a fatigue stage, when shutting down the hydraulic press.

The experiment could consist in applying a variable force with the hydraulic pulsator at certain constant frequency, decreasing progressively the tension and intrinsic mean stress, possibly dividing it in stages. Thus, with an accelerometer and a potentiometer to measure frequencies and deflections, and the pressure plate to measure the tension at each moment, it is possible to test such effects and calibrate to avoid under or over estimations.

8. Conclusions

The main contribution of this manuscript is to rethink the mean stress during fatigue life, dividing it into two components by source: extrinsic and intrinsic mean stresses, disclosing their implications. Besides, it defines a new mean stress pushing factor on the basis of Goodman equation, to be applied after the histogram is found. Moreover, three second-order fatigue effects derived from intrinsic mean tension are also identified and described: cycle quasi-order, histogram variation and apparent mean tension. Finally, as a case study a CBF system of 12 DOF is used disclosing the procedure to take into account each part of mean stress.

1. The concepts of *extrinsic* and *intrinsic* mean stress have been presented. *Extrinsic* mean stress arises from the actual variable random loading that causes fatigue, while *intrinsic* mean stress is due to concomitant permanent loads or indirect structural responses, not directly related to the random loading.
2. *Extrinsic* mean stress can be considered for any stress range, $\Delta\sigma$, based on the fatigue damage forecast method, modified by an innovative mean stress pushing factor, F_{MSP}, derived from Goodman's ratio, as long as the cycle counting method that is employed registers such information in the same way as the Rainflow method.
3. The same applies to *intrinsic* mean stress, although intrinsic mean stress usually arises from an existing concomitant tension tending to slowly decrease with time, while that tension causes three *second-order fatigue effects*, increasing expectable damage and must, therefore, be considered.
4. The first second-order fatigue effect identified in this study is the *cycle quasi-ordering*, occurring when a random loading, defined as an stochastic stationary and ergodic process, is concomitant to a slowly varying mean tension. In such cases, the equivalent range, $\Delta\sigma_{eq}$, at 0-mean stress, $\sigma_m = 0$, will tend to be greater in earlier cycles than in later ones. As this amplification is verified and applied simultaneously to all the harmonics

in the stochastic process, then it is likewise for the summation by the distributive property.

5. The second second-order fatigue effect is the *histogram modification*. It occurs because any existing tension changes the structural system effective stiffness and, therefore, the natural frequencies and the Frequency Response Functions (FRF) will vary accordingly. Besides, it implies a change in the response power spectra, $S_y(f)$, and the corresponding cycle counting. Moreover, as the tension tends to vary during the service life, the natural frequencies could become coupled to those of the input power spectra, causing resonance and near resonance effects at that time.
6. The third second-order fatigue effect is the generation of an apparent mean stress, due to the unloading of some elements under compression, because of buckling, transferring such loading to other elements under tension.
7. A case study based on the bracing system of a 12-storey building under wind loading has been developed, showing how to take into account the above-mentioned second-order effects and how to integrate their impact on fatigue calculations.

9. Acknowledgements

The authors would like to thank and extend their warm recognition to Mr. Asier Maiztegi Eriz, for establishing and managing the framework within Tecnalia that made the PhD Thesis possible that is summarized in this paper. (Thank you Asier, you were not the only one with eyes, but certainly the only one with a view).

References

References

[1] W. Erickson, C. E. Work, A study of the accumulation of fatigue damage in steel, in: Proceedings of American Society of Testing Materials, 1961, pp. 704–718.

[2] V. Bhandari, Design of Machine Elements, Tata McGraw-Hill, 2010.

[3] J. Goodman, Mechanics Applied to Engineering, Longmans, Green & Company, 1899.

[4] W. Gerber, Calculation of allowable stresses in iron structures, Bayer ArchitIngVer 6 (6) (1874) 101–110.

[5] C. Soderberg, Factor of safety and working stress, Trans ASME 52-2 (1930) 13–28.

[6] A. Palmgren, Die lebensdauer von kugellagern, Zeitschrift des Vereins Deutscher Ingenieure 68 (14) (1924) 339–341.

[7] M. Miner, Cumulative damage in fatigue, Journal of Applied Mechanics 12 (3) (1945) A159–A164.

[8] A. Wöhler, über die festigkeitsversuche mit eisen und stahl, Zeitschrift fr Bauwesen 20 (1870) 73–106.

[9] B. S. Institution, BS EN 1993-1-1:2005+A1:2014. Eurocode 3. Design of steel structures. General rules and rules for buildings (2014).

[10] B. S. Institution, BS EN 1993-1-8: 2005. Eurocode 3. Design of Steel Structures. Design of Joints (2005).

[11] B. S. Institution, BS EN 1993-1-9:2005 Eurocode 3. Design of steel structures. Fatigue (2005).

[12] E. C. for Constructional Steelwork, Document 43 - Recommendations for the fatigue design of steel structures, ECCS European Convention for Constructional Steelwork, Brussels, Belgium, 1st Edition (1985).

[13] A. 7-10, Minimum Design Loads for Buildings and Other Structures, Structural Engineering Institute, United States of America (2010).

[14] A. 341-10, Seismic Provisions for Structural Steel Buildings (ANSI/AISC 341-10), AISC, United States of America, 3rd Edition (September 2012).

[15] A. 360-16, Specification for Structural Steel Buildings, AISC, United States of America (2016).

[16] AASHTO, LRFD Bridge design specifications, American Association of State Highway and Transportation Officials, Washington DC, USA, 5th Edition (2010).

[17] AASHTO, The Manual for bridge evaluation, American Association of State Highway and Transportation Officials, Washington DC, USA, 1st Edition (2008).

[18] O. Basquin, The exponential law of endurance tests, Proc Am Soc Test Mater 10 (1910) 625–630.

[19] P. Paris, F. Erdogan, A critical analysis of crack propagation laws, Journal of Fluids Engineering, Transactions of the ASME 85 (4) (1963) 528–533. doi:10.1115/1.3656900.

[20] A. Griffith, The Phenomena of Rupture and Flow in Solids, Philosophical transactions / Royal Society of London, 1920.

[21] G. Irwin, Analysis of stresses and strains near the end of a crack traversing a plate. j appl mech trans asme 24: 361-364, Journal of Applied Mechanics 24 (1957) 361–364.

[22] Y. Choi, D. J. Oh, J. M. Lee, K. S. Lee, M. H. Kim, A new model of fatigue crack growth rate considering mean stress effects due to locked-in stress, International Journal of Steel Structures 19 (4) (2019) 1099–1111. doi:10.1007/s13296-018-0190-z.
URL https://doi.org/10.1007/s13296-018-0190-z

[23] K. R. Chandran, Fatigue crack growth in bending: Successful correlation of mean stress (stress ratio) effects using the change in net-section strain energy, Fatigue & Fracture of Engineering Materials & Structures 41 (12) (2018) 2566–2576.

arXiv:https://onlinelibrary.wiley.com/doi/pdf/10.1111/ffe.12857,
doi:10.1111/ffe.12857.
URL https://onlinelibrary.wiley.com/doi/abs/10.1111/ffe.12857

[24] B. S. Institution, BS EN 1991-1-1:2002 Eurocode 1. Actions on structures. General actions. Densities, self-weight, imposed loads for buildings (2002).

[25] S. Timoshenko, J. Goodier, Theory of Elasticity, by S. Timoshenko and J.N. Goodier, ... 2nd Edition, McGraw-Hill Book Company, 1951.

[26] M. Matsuishi, T. Endo, Fatigue of metals subjected to varying stress, Japan Society of Mechanical Engineers, Fukuoka, Japan 68 (2) (1968) 37–40.

[27] N. Dowling, Fatigue failure predictions for complicated stress-strain histories, J. Mater. 7 (1971) 88.

[28] R. Anthes, Modified rainflow counting keeping the load sequence, International Journal of Fatigue 19 (7) (1997) 529 – 535. doi:https://doi.org/10.1016/S0142-1123(97)00078-9.

[29] K. Dressler, M. Hack, W. Krger, Stochastic reconstruction of loading histories from a rainflow matrix, Zamm-zeitschrift Fur Angewandte Mathematik Und Mechanik 77 (1997) 217–226. doi:10.1002/zamm.19970770315.

[30] S. Downing, D. Socie, Simple rainflow counting algorithms, International Journal of Fatigue 4 (1) (1982) 31 – 40. doi:https://doi.org/10.1016/0142-1123(82)90018-4.

[31] A. E1049, Standard Practice for Cycle Counting in Fatigue Analysis (1999).

[32] ESDU 95006 A-1995 Fatigue life estimation under variable amplitude loading using cumulative damage calculations (1995).

[33] C. Amzallag, J. Gerey, J. Robert, J. Bahuaud, Standardization of the rainflow counting method for fatigue analysis, International Journal of Fatigue 16 (4) (1994) 287 – 293. doi:https://doi.org/10.1016/0142-1123(94)90343-3.

[34] I. Rychlik, A new definition of the rainflow cycle counting method, International Journal of Fatigue 9 (2) (1987) 119 – 121. doi:https://doi.org/10.1016/0142-1123(87)90054-5.

[35] D. Benasciutti, Fatigue analysis of random loadings, Ph.D. thesis, University of Ferrara (2004).

[36] D. Benasciutti, R. Tovo, Modelli di previsione del danneggiamento a fatica per veicoli in regime stazionario ed ergodico, 2002.

[37] R. Tovo, Cycle distribution and fatigue damage under broad-band random loading, International Journal of Fatigue 24 (2002) 1137–1147. doi:10.1016/S0142-1123(02)00032-4.

[38] M. Mrnik, J. Slavi, M. Boltear, Frequency-domain methods for a vibration-fatigue-life estimation application to real data, International Journal of Fatigue 47 (2013) 8 – 17. doi:https://doi.org/10.1016/j.ijfatigue.2012.07.005.
URL http://www.sciencedirect.com/science/article/pii/S0142112312002320

[39] R. Clough, J. Penzien, Dynamics of Structures, McGraw-Hill, 1993.
URL https://books.google.es/books?id=HxLakQEACAAJ

[40] D. Thorby, Structural Dynamics and Vibration in Practice: An Engineering Handbook, Elsevier Science, 2008.
URL https://books.google.es/books?id=PwzDuWDc8AgC

[41] G. Maymon, Structural Dynamics and Probabilistic Analysis for Engineers, Elsevier Science, 2008.
URL https://books.google.es/books?id=hNqJavUZ9TQC

[42] Z. Wu, Y. Zhao, J. Liang, M. Fu, G. Fang, A frequency domain approach in residual stiffness estimation of composite thin-wall structures under random fatigue loadings, International Journal of Fatigue 124 (2019) 571 – 580. doi:https://doi.org/10.1016/j.ijfatigue.2019.03.013.
URL http://www.sciencedirect.com/science/article/pii/S0142112318307308

[43] D. P. Kihl, S. Sarkani, Mean stress effects in fatigue of welded steel joints, Probabilistic Engineering Mechanics 14 (1) (1999) 97 – 104. doi:https://doi.org/10.1016/S0266-8920(98)00019-8.
URL http://www.sciencedirect.com/science/article/pii/S0266892098000198

[44] A. Nieslony, M. Böhm, Mean stress effect correction using constant stress ratio sn curves, International Journal of Fatigue 52 (2013) 49 – 56. doi:https://doi.org/10.1016/j.ijfatigue.2013.02.019.
URL http://www.sciencedirect.com/science/article/pii/S0142112313000686

[45] A. Ince, G. Glinka, A modification of morrow and smithwatsontopper mean stress correction models, Fatigue & Fracture of Engineering Materials & Structures 34 (2011) 854–867. doi:10.1111/j.1460-2695.2011.01577.x.

[46] O. Karakas, Consideration of mean-stress effects on fatigue life of welded magnesium joints by the application of the smithwatsontopper and reference radius concepts, International Journal of Fatigue 49 (2013) 1 – 17. doi:https://doi.org/10.1016/j.ijfatigue.2012.11.007.
URL http://www.sciencedirect.com/science/article/pii/S0142112312003398

[47] N. Apetre, A. Arcari, N. Dowling, N. Iyyer, N. Phan, Probabilistic model of mean stress effects in strain-life fatigue, Procedia Engineering 114 (2015) 538 – 545, iCSI 2015 The 1st International Conference on Structural Integrity Funchal, Madeira, Portugal 1st to 4th September, 2015. doi:https://doi.org/10.1016/j.proeng.2015.08.103.
URL http://www.sciencedirect.com/science/article/pii/S1877705815017427

[48] M. Morgantini, D. MacKenzie, T. Comlekci, R. van Rijswick, The effect of mean stress on corrosion fatigue life, Procedia Engineering 213 (2018) 581 – 588, 7th International Conference on Fatigue Design, Fatigue Design 2017, 29-30 November 2017, Senlis, France. doi:https://doi.org/10.1016/j.proeng.2018.02.053.
URL http://www.sciencedirect.com/science/article/pii/S1877705818302844

[49] I. Calderon-Uriszar-Aldaca, M. Biezma, A plain linear rule for fatigue analysis under natural loading considering the sequence effect, International Journal of Fatigue 103 (2017) 386–394. doi:10.1016/j.ijfatigue.2017.06.018.

[50] I. Calderon-Uriszar-Aldaca, E. Briz, M. Biezma, I. Puente, A plain linear rule for fatigue analysis under natural loading considering the coupled fatigue and corrosion effect, International Journal of Fatigue 122 (2019) 141–151. doi:10.1016/j.ijfatigue.2019.01.008.

[51] I. Calderon-Uriszar-Aldaca, Fatigue of structural elements by random dynamic actions in aggressive environment, Ph.D. thesis, ETS Ingenieros de Caminos, Canales y Puertos, Universidad de Cantabria (2014).

[52] A. Nieslony, M. Böhm, Frequency-domain fatigue life estimation with mean stress correction, International Journal of Fatigue 91 (2016) 373 – 381, variable Amplitude Loading. doi:https://doi.org/10.1016/j.ijfatigue.2016.02.031.
URL http://www.sciencedirect.com/science/article/pii/S0142112316000803

[53] A. Nieslony, M. Böhm, Mean stress effect correction in frequency-domain methods for fatigue life assessment, Procedia Engineering 101 (2015) 347 – 354, 3rd International Conference on Material and Component Performance under Variable Amplitude Loading, VAL 2015. doi:https://doi.org/10.1016/j.proeng.2015.02.042.
URL http://www.sciencedirect.com/science/article/pii/S1877705815006402

[54] A. Nieslony, M. Böhm, Mean stress value in spectral method for the determination of fatigue life, Acta Mechanica et Automatica 6 (2012) 71–74.

[55] H. J. Sutherland, J. F. Mandell, The effect of mean stress on damage predictions for spectral loading of fibreglass composite coupons, Wind Energy 8 (2005) 93 – 108. doi:10.1002/we.125.

[56] M. Kamaya, M. Kawakubo, Mean stress effect on fatigue strength of stainless steel, International Journal of Fatigue 74 (2015) 20 – 29.

doi:https://doi.org/10.1016/j.ijfatigue.2014.12.006.
URL http://www.sciencedirect.com/science/article/pii/S014211231400317X

[57] B. Standard, Eurocode 8: Design of structures for earthquake resistance (2005).

[58] H. Degée, C. Castiglioni, A. Kanyilmaz, I. Calderon, P.-O. Martin, Design of concentrically braced frames for optimized performances in moderate earthquake areas, 2016.

[59] B. S. Institution, BS EN EN 1991-1-4 Eurocode 1: Actions on structures, general actions part 14. Wind actions (2005).

[60] A. Davenport, The spectrum of horizontal gustiness near the ground in high winds, Quarterly Journal of the Royal Meteorological Society 88 (1962) 197–198. doi:10.1002/qj.49708837618.

[61] W. Zhao, M. J. Baker, On the probability density function of rainflow stress range for stationary gaussian processes, International Journal of Fatigue 14 (2) (1992) 121 – 135. doi:https://doi.org/10.1016/0142-1123(92)90088-T.
URL http://www.sciencedirect.com/science/article/pii/014211239290088T

[62] G. Petrucci, B. Zuccarello, Fatigue life prediction under wide band random loading, Fatigue & Fracture of Engineering Materials & Structures 27 (2004) 1183 – 1195. doi:10.1111/j.1460-2695.2004.00847.x.

[63] L. Lutes, M. Corazao, S. James Hu, J. J. Zimmerman, Stochastic fatigue damage accumulation, Journal of Structural Engineering 110 (1984) 2585–2601. doi:10.1061/(ASCE)0733-9445(1984)110:11(2585).

[64] J. Ding, X. Chen, Fatigue damage evaluation of broad-band gaussian and non-gaussian wind load effects by a spectral method, Probabilistic Engineering Mechanics 41 (2015) 139 – 154. doi:https://doi.org/10.1016/j.probengmech.2015.06.005.
URL http://www.sciencedirect.com/science/article/pii/S0266892015300230

[65] T. Dirlik, Application of computer in fatigue analysis, Ph.D. thesis (01 1985).

[66] C. Braccesi, F. Cianetti, L. Tomassini, Random fatigue. a new frequency domain criterion for the damage evaluation of mechanical components, International Journal of Fatigue 70 (2015) 417 – 427. doi:https://doi.org/10.1016/j.ijfatigue.2014.07.005.
URL http://www.sciencedirect.com/science/article/pii/S0142112314002011

[67] J. S. Bendat, A. G. Piersol, Random data: analysis and measurement procedures, Vol. 729, John Wiley & Sons, 2011.

[68] S. M. Ross, Introduction to probability and statistics for engineers and scientists, Academic Press, 2014.

[69] V. Bouyssy, S. Naboishikov, R. Rackwitz, Comparison of analytical counting methods for gaussian processes, Structural Safety 12 (1) (1993) 35 – 57. doi:https://doi.org/10.1016/0167-4730(93)90017-U.
URL http://www.sciencedirect.com/science/article/pii/016747309390017U

[70] N. Bishop, Spectral methods for estimating the integrity of structural components subjected to random loading, in: Handbook of fatigue crack propagation in metallic structures, Elsevier, 1994, pp. 1685–1720.

[71] A. Halfpenny, A frequency domain approach for fatigue life estimation from finite element analysis, Key Engineering Materials - KEY ENG MAT 167-168 (1999) 401–410. doi:10.4028/www.scientific.net/KEM.167-168.401.

Highlights

- Mean stress pushing factor to fatigue damage
- Consideration of intrinsic and extrinsic mean stress
- Definition of three second-order fatigue effects
- Development of a 12-storey building as case study
- Proposition of a simple experimental setup